The Nature of the Inputs to Cortical Motion Detectors

LEONID L. KONTSEVICH*

Recently, Jagadeesh, Wheat and Ferster [(1993) *Science*, *262*, 1901–1904] presented intracellular recordings from direction-selective simple cells in primary visual cortex and provided an analysis to support the idea that synaptic summation in simple cells is linear. New analysis presented in this study reveals that: (1) the number of subunits contributing to the analyzed simple cell inputs is two; (2) the subunits are nonlinear in the time domain; (3) each subunit linearly integrates the luminance across the receptive field being, thus, linear to local contrast; (4) the waveforms of the subunit signals are linearly modulated by local contrast at the subunit loci unless the contrast changes its sign; (5) the synaptic summation in the simple cell is linear; (6) nonlinearity of even harmonics has sufficient information for retrieving of relative spatial phase of the subunits and reconstruction of the exact temporal profiles of the subunit signals.

Motion   Motion selectivity   Motion subunits   Simple cell   Cortex   Intracellular

INTRODUCTION

An important problem for contemporary visual neurophysiology is to describe the transformations that the signals undergo at the initial stages of visual processing. Its solution requires identification of the interneural connections and properties of each neuron involved in the processing. Although the behavior of a large number of neurons has been described and classified, there is still much to do in analyzing these data due to the enormous number of interneural connections and the nonlinearities of signal transmission.

There is, however, an analytical approach to the problem of neural transmission properties: to record the responses of a particular neuron to a representative set of stimuli and derive the underlying structure analytically. This approach works well for linear systems although neurons demonstrate nonlinear behavior. In this study I demonstrate that, despite some nonlinear features of the signal transfer, the analytical approach may be applied to physiological recordings, such as those of Jagadeesh, Wheat and Ferster (1993) from simple directionally selective cells of cat area 17, to provide important information about the neural circuitry underlying the intracellular potentials.

The experimental paradigm used by Jagadeesh *et al.* (1993) was based on the mathematical identity that a drifting sinusoidal grating can be represented as a linear sum of several stationary contrast-modulated gratings with a proper relation between spatial and temporal phases. The authors demonstrated that, for *intra-*

cellularly recorded membrane potentials in a direction-selective simple cell, linear additivity holds. When the cell responses to stationary gratings with different spatial phases were added with proper temporal phases, their sum closely matched the directly measured response to the drifting grating. The computed sums for drift in the preferred and nonpreferred directions had different amplitudes, just as observed in the recordings of membrane potential. This finding is especially important in the light of previous studies that failed to support the presence of such linearity in *extracellular* responses (Albrecht & Geisler, 1991; Emerson, Citron, Vaughn & Klein, 1987; Ganz & Felder, 1984; Reid, Soodak & Shapley, 1991; Tolhurst & Dean, 1991), apparently due to an accelerating or threshold nonlinearity in the spike generation process. Thus, the methodological advance of cortical intracellular recording introduced by Jagadeesh *et al.* (1993) allowed them to reveal linear properties preceding spike generation nonlinearity.

The main conclusion of Jagadeesh *et al.* (1993) was that the synaptic summation in simple cells is linear although they did not evaluate the cells' linearity with respect to contrast, time and space. The fuller analysis presented below solidifies and elaborates the statements about linearity, revealing a number of properties in addition to those mentioned in the original study. The approach developed here is based on formal tests of linearity without inclusion of any physiological presuppositions in the analysis. It will be shown that:

(1) the analyzed cell receives signals from two independent sources (i.e. two physiological subunits);
(2) both subunit responses are nonlinear with respect to time (i.e. nonsinusoidal for a sinusoidal input);

*Smith-Kettlewell Eye Research Institute, 2232 Webster Street, San Francisco, CA 94115, U.S.A.

(3) each subunit linearly integrates the luminance across the receptive field (i.e. for periodic stimuli the subunit has no output signal at certain spatial phases);

(4) the nonlinear profile of the subunit response is linearly modulated by the local contrast in the subunit receptive field;

(5) summation of the subunit signals (synaptic summation) in the simple cell is linear;

(6) nonlinearity of even harmonics has sufficient information for retrieving of relative spatial phase of the subunits and reconstruction of the exact temporal profiles of the subunit signals.

THE DATA

The data curves from Jagadeesh et al. (1993, Fig. 1A) were scanned, digitized by DataThief (Huyser, K. & van der Laan, J. B., NIKHEF-K, Amsterdam, The Netherlands) with a sampling frequency of 180 points per curve and subsequently analyzed in MatLab[tm] (MathWorks, Inc., Natick, Mass.). In the present analysis [see Fig. 1(A)], each curve represents one period (500 msec) of the membrane potential modulation evoked by a counterphase oscillating sinusoidal grating presented at a particular spatial phase. The spatial frequency of the 60% contrast grating was adjusted at the beginning of the experiment to evoke the strongest response to 2 Hz motion (D. Ferster, personal communication).

FACTOR ANALYSIS

To determine the factors contributing to the data, a singular value decomposition was performed for an 8 × 180 matrix comprised of eight sets of 180 sampled points for each recording in Fig. 1(A) with the d.c. components eliminated. The set of singular values (weights of the orthogonal factors) was: 5.82, 2.95, 0.50, 0.35, 0.27, 0.16, 0.15, 0.14. The first two are the values of the same order, while the ratio between the second and the third (5.9) is much larger than the ratios between the first two or between the further subsequent pairs of eigenvalues. Therefore the data set is essentially two-dimensional; the first two factors account for 98.8% of the overall variance in the data. We can conclude that the membrane potentials in the analyzed simple cell can be described using only two independent factors whose waveforms are combined linearly to form the cell's membrane potential.

The prediction of the linear two-factor model presented in Fig. 1(B) captures most of the features of the analyzed data. The only salient feature that seems to be lost in the prediction of this two-factor model is a small bump toward the right for spatial phases 135 and 157.5 deg; this feature will be recaptured in the final version of the model.

The success of the two-factor linear model validates the conclusion of Jagadeesh et al. (1993, Fig. 1A) that the summation of the input signals in the simple cell is linear. The next conclusion is related to the number of
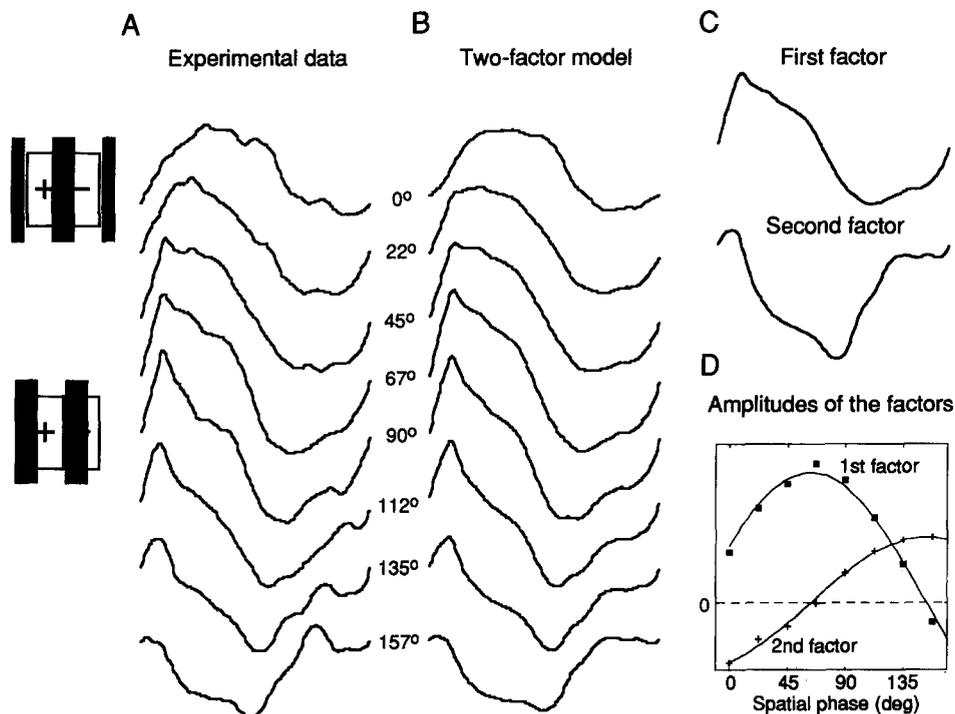

FIGURE 1. (A) The original data scanned from Fig. 1(A) in Jagadeesh et al. (1993). Each curve represents the intracellular response of the directional simple cell to counterphase flicker (2 Hz) of a stationary sinusoidal grating (contrast 60%) in the specific spatial phase shown on the left. The units of the response are arbitrary but the same across all recordings. (B) The data fit by two-factor model that accounts for 98.8% of the data variance. All the curves constitute a two-dimensional space. (C) The two main factors of the model. These factors constitute some orthogonal basis in the two-dimensional space of the response profiles. (D) The amplitudes of two main factors vs spatial phase (amplitude units are arbitrary). Good fit to sinusoidal variation indicates linearity of the subunits to local contrast.
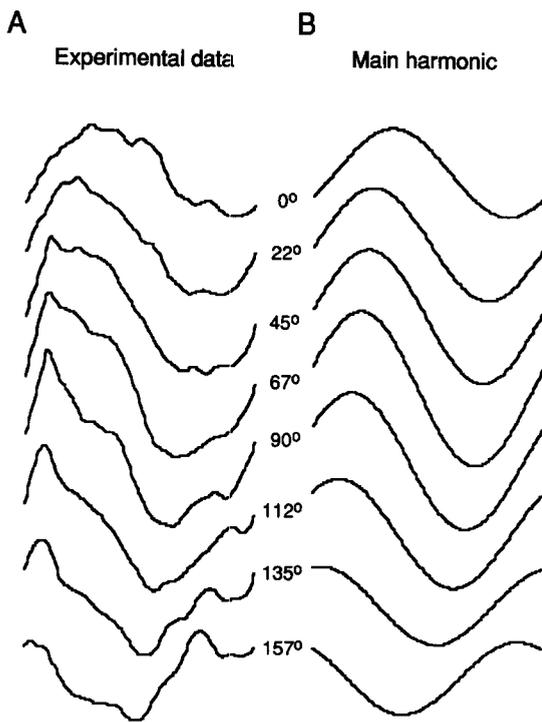
A
Experimental data

B
Main harmonic

FIGURE 2. (A) Data replotted from Fig. 1(A). (B) The fundamental harmonic of the data accounts for 92.8% of the data variance. The significant deviation of the response waveforms from the fundamental sinusoids indicates nonlinearity in the simple cell responses in time domain.

the spatially separate subunits which provide the inputs to the simple cell.

One could attribute the two independent factors to the fundamental (2 Hz) harmonic of the responses alone because the amplitude and phase at a given frequency constitute a two-dimensional space. Following this logic, the two-factor model does not constrain the number of the subunits because the sum of any number of sinusoidal waveforms is sinusoidal. That would be correct if the subunits were linear in the temporal domain; i.e. the sinusoidal signal at the subunit input would evoke the sinusoidal signal of the same frequency at its output. The simple cell behavior, however, is markedly nonlinear: the recordings [Fig. 1(A)] strongly deviate from sinusoidal profiles although the temporal modulation of the stimulus was sinusoidal. The fundamental shown in Fig. 2 accounts only for 92.8% of the signal variance. The remaining 7.2% of the signal variance is due to the nonlinear component of the simple cell response; the linear two-factor model accounts for 83.8% of this residual variance, which is a high level considering the inevitable presence of noise in the recordings.

The nonlinear component of the signal is the sum of all high harmonics (all except the fundamental). The higher harmonics add new independent dimensions to the signal space and impose additional constraints on the two-factor model. The fact that the model matches these constraints with good precision means that the analyzed simple cell gets inputs from two spatially independent sources of information that may be conceptualized as physiological subunits. (Note that, in principle, three or

more independent sources may coincidentally fit a two-factor model. The probability of such a coincidence, however, is vanishingly small for 180-dimensional data set.)

Thus, (1) the simple cell receives signals from two subunits and (2) the synaptic summation of the subunit signals is highly linear. The first conclusion is consonant with the two-subunit assumption embodied in all motion-detection models (Adelson & Bergen, 1985; Reichardt, 1961; van Santen & Sperling, 1985; Watson & Ahumada, 1985). The second conclusion, which is in agreement with the claim of linear summation in Jagadeesh et al. (1993), lends it greater support because in our case the linear combination rule holds for all eight data curves vs two curves in Jagadeesh et al. (1993).

LINEAR MODEL

Although the two-factor model implies that the factor weights are somehow related to spatial phase of the test grating, it does not provide the exact relation. This issue is addressed by a linear model that constrains the amplitudes of the two factors for each waveform to be linear with respect to local contrast.

The main factors of the two-factor model [Fig. 1(C)] are each a weighted sum of the subunit signals. In this sense these factors exist as abstractions, and the fact that they are orthogonal does not imply the presence of the quadrature relations between the subunits. Empirically, the factors' amplitudes vary nearly sinusoidally with spatial phase as shown in Fig. 1(D). This property indicates that the subunits are linear to local contrast: the magnitude of the signal at the subunit output is linearly proportional to the magnitude of the contrast oscillation in the receptive field of the subunit. The linear model provides a rigorous test of contrast linearity.

For sinusoidal gratings, contrast linearity means that the signal from each subunit is proportional to $\sin(\chi - \varphi)$, were φ is the grating phase and χ is the subunit phase. Thus, the simple cell response $S_\varphi(t)$ to the counterphase oscillating grating with spatial phase φ is:

$$S_\varphi(t) = \sin(\chi_1 - \varphi)S_1(t) + \sin(\chi_2 - \varphi)S_2(t) \qquad (1)$$

where χ_1 and χ_2 here are the positions of the subunits; $S_1(t)$ and $S_2(t)$ are the signal profiles for the subunits. Each of the coefficients in equation (1) can be decomposed into the weighted sum of $\sin(\varphi)$ and $\cos(\varphi)$. After this substitution we arrive at

$$S_\varphi(t) = \sin(\varphi)A(t) + \cos(\varphi)B(t) \qquad (2)$$

where $A(t)$ and $B(t)$ are some weighted sums of the subunit temporal profiles (we are not interested at this point in the particular weights). The coefficients now are independent of the unknown spatial phases of the subunits.

Because for every data curve the phase φ is determinate, equation (2) can be treated as a linear equation on the unknowns $A(t)$ and $B(t)$. Eight data curves comprise a highly overdetermined linear system of eight equations which has been solved to obtain $A(t)$ and $B(t)$.
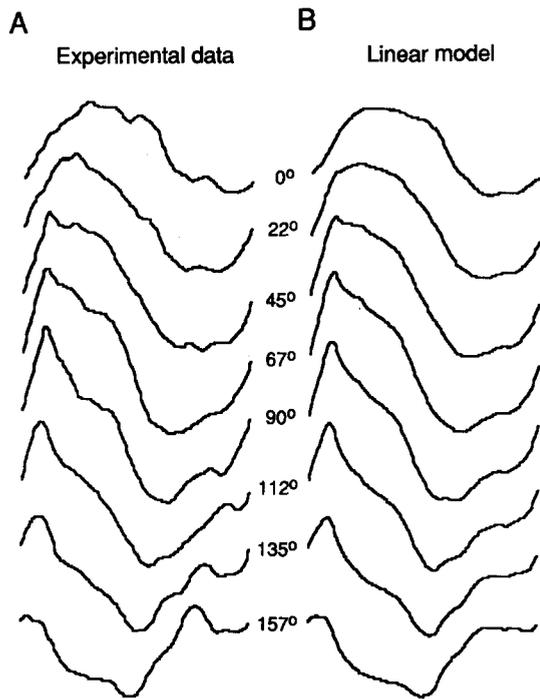
FIGURE 3. (A) Data replotted from Fig. 1(A). (B) The prediction of the linear model where the amplitudes of two factors are constrained by the spatial phase. The precision of the linear model (98.3%) is almost as good as the precision of two-factor model (98.8%), where the amplitudes are not constrained.
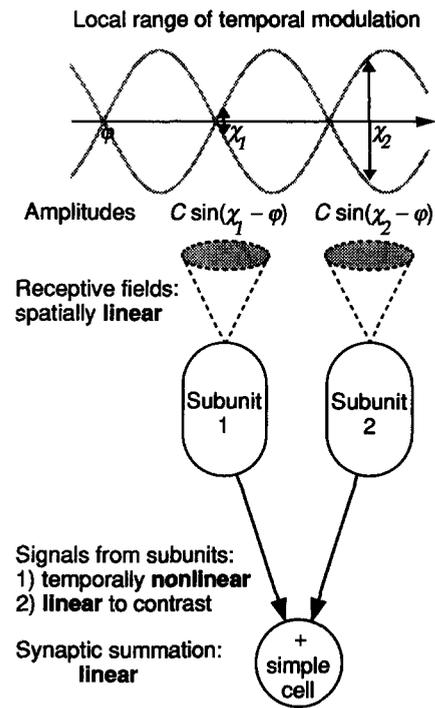
FIGURE 4. Block diagram of the linear model. The signals arrive at the simple cell from two subunits. The summation of these signals in the simple cell is *linear*. The temporal profiles of the subunit signals are *nonlinear*; although the amplitude of the signal from each subunit *linearly* depends on the temporal modulation amplitude in the corresponding receptive field which is a function of the test grating the phase φ and subunit spatial location χ. Contrast linearity implies that each subunit is *linear* in the spatial domain.

These $A(t)$ and $B(t)$ being combined by equation (2) comprise the predictions of the linear model shown in Fig. 3.

This linear model constrains the amplitudes of the two factors; it is much more restrictive than the previous two-factor model where these amplitudes are free parameters. Despite this difference the linear model accounted for 98.3% of the data variance, which is close to the 98.8% obtained with the two-factor model. Such a high accuracy for the linear model indicates that the subunits are highly linear to the local contrast, which ranged between 0% and 60% as spatial phase varied.

Contrast linearity of the subunits implies, according to equation (1), that at certain spatial phases of the test grating the subunits do not respond to the flicker. This property indicates in turn that the subunits are spatially linear (Enroth-Cugell & Robson, 1966). If a subunit incorporates several smaller LGN receptive fields, as Hubel and Wiesel (1962) suggested, then the LGN cells providing inputs for a particular subunit must have the same temporal nonlinearity; otherwise this nonlinearity will depend on spatial phase and contrast linearity will fail.

The results of the previous analysis are summarized in Fig. 4. The temporally nonlinear outputs of two subunits have stable shapes that are linearly modulated by the amplitude of the oscillations in the subunit receptive fields. These signals are combined in the simple cell by a linear summation rule.

QUASILINEAR MODEL

Although the data set presented in Jagadeesh *et al.* (1993, Fig. 1A) covers only half (0–180 deg) of the possible range of spatial phases, it easily can be extended to the full range (0–360 deg). Consider how the response for the spatial phase φ is related to the response for $\varphi + 180$ deg. The input modulation can be expressed as $L_0(1 + C \sin(2\pi f_s x - \varphi) \cdot \sin(2\pi f_t t))$ where f_s and f_t are the spatial and temporal frequencies of the modulation, x is a space coordinate, t is time. Since $\sin(2\pi f_s x - \varphi - \pi) \cdot \sin(2\pi f_t t) = -\sin(2\pi f_s x - \varphi)$ $\cdot \sin(2\pi f_t t) = \sin(2\pi f_s x - \varphi) \cdot \sin(\pi + 2\pi f_t t)$, the response at spatial phase $\varphi + 180$ deg exactly matches the response for the spatial phase φ shifted by a half-period in the temporal domain. The extended data set obtained with this procedure is shown in Fig. 5(A). The linear model was designed with no restrictions on the range of spatial phases; however, when applied to the extended data set, this model produced relatively poor fit with a residual variance of 3.9% vs 1.7% for the 0–180 deg range [see Fig. 5(B)].

One problem with the linear model is that the temporal nonlinearity does not behave exactly linearly with respect to local contrast; this important factor was not considered earlier for sake of simplicity. A *quasilinear model* that captures this omission and avoids the degraded fit for the full spatial range will now be developed [the quasilinear fit is presented for comparison in Fig. 5(C)].

A
Experimental data
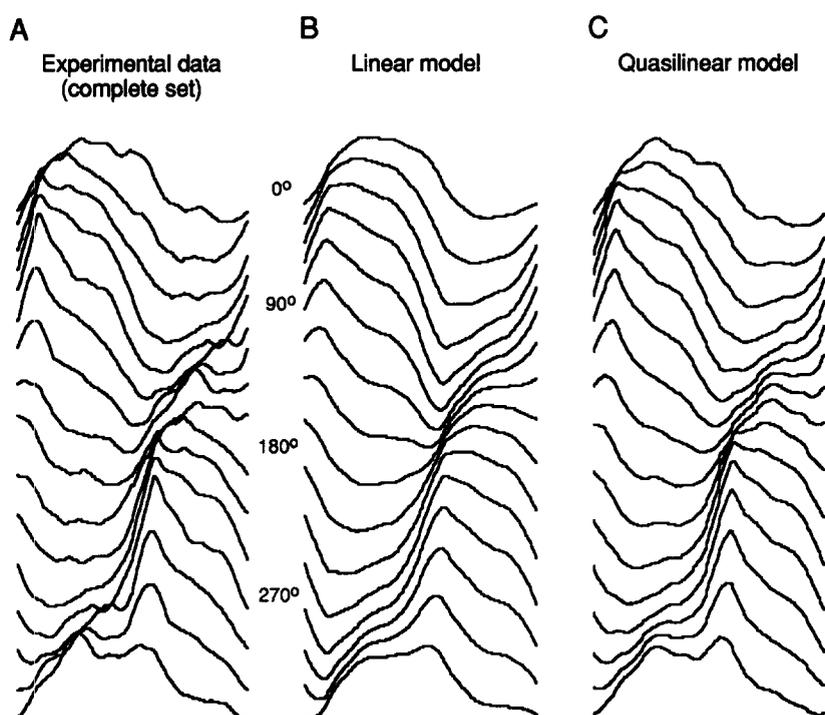(complete set)

B
Linear model

C
Quasilinear model

FIGURE 5. (A) Extended set of response waveforms. The curves for the spatial phases of 0–157.5 deg are the original data from Fig. 1(A); the responses for 180–337.5 deg are obtained by shifting the same curves by 180 deg of the fundamental. (B) Prediction of the linear model for the extended data set. The precision of the linear model for full range of spatial phases is 96.1%. (C) Prediction of the quasilinear model which takes into account the asymmetry between positive and negative waveforms and accounts for 98.7% of the data variance. The residual variance of the quasilinear model is 3 times lower than for the linear model.

The nonlinearity in the analyzed data distorts positive and negative half-periods differently; otherwise, both half-periods in the recordings from Fig. 1(A) would be of the same shape. This difference means that a sign-asymmetric nonlinearity is present in at least one of the subunits. Such a nonlinearity is inconsistent with the notion of contrast linearity of the subunits. At the beginning of this section it was established that a 180 deg spatial phase shift of the test grating leads to a 180 deg phase shift of the output signal in time, which is not equivalent to sign inversion of the output signal because of the asymmetry between the positive and negative lobes of the waveform. In mathematical terms, the 180 deg phase shift in space transforms the signal $S(t)$ into $S(t + T/2)$, (where $T = 500$ msec is the modulation period), which is not equal to the $-S(t)$ predicted by the linear model. A simple example of such nonlinear behavior is a half-wave rectifier (see Fig. 6).

Spatial phase shifts do not affect the temporal phase of the subunit response unless the spatial phase goes through the subunit null point. Thus, between its null-points each subunit is linear to contrast. The nonlinearity appears across the null-points where odd and even harmonics of the signal behave differently: odd harmonics invert the sign whereas even harmonics sustain it, as is illustrated in Fig. 7. Thus, odd harmonics respond to the contrast sign change linearly across the whole range

of contrasts and even harmonics are linear only in the subranges between null-points.*

The odd component $P_\varphi(t)$ of the simple cell response (the sum of all odd harmonics) is spatially linear:

$$P_\varphi(t) = \sin(\chi_1 - \varphi)P_1(t) + \sin(\chi_2 - \varphi)P_2(t) \quad (3)$$

where $P_1(t)$ and $P_2(t)$ are the odd components of the temporal responses of the subunits. The even component $Q_\varphi(t)$ of the modulation is linear between null-points:

$$Q_\varphi(t) = |\sin(\chi_1 - \varphi)|Q_1(t) + |\sin(\chi_2 - \varphi)|Q_2(t). \quad (4)$$

The full response of the simple cell is given by the sum of its odd and even components:

$$S_\varphi(t) = P_\varphi(t) + Q_\varphi(t). \quad (5)$$

The analyzed data indeed demonstrate the difference between the behavior of the odd and even components as illustrated in Fig. 8(B, C). The odd component features change their sign across the spatial phases; the features from even harmonics do not change sign. For the even component [Fig. 8(C)] the peak 1S is present at all spatial phases and disappears somewhere between 0 and 22.5 deg (and correspondingly between 180 and 202.5 deg). The similar peak marked 2S disappears in the range between 45 and 112.5 deg. These eyeball estimates are shown by the segments with arrows at the ends. The specified peaks obviously originate from different subunits because the spatial phases of the null-points are clearly different.

Equation (3), being spatially linear, does not constrain the subunit phases, while equation (4) provides such

---

*Spitzer and Hochstein (1985) were the first to notice the sign stability of even harmonics for the case of rectifying nonlinearity. In fact, this property is valid for any temporal nonlinearity.

Temporally
modulated
input
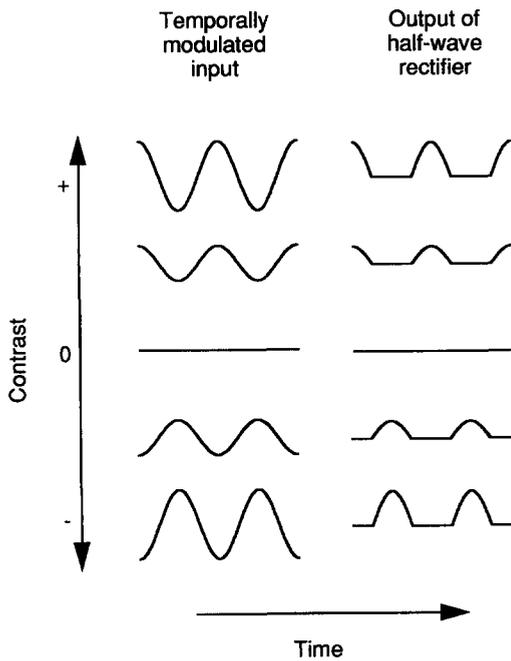
Output of
half-wave
rectifier

FIGURE 6. The nonlinear phase-shift effect for the case of a half-wave rectifier. The left column represents the temporal input for the half-wave rectifier. The corresponding outputs of the rectifier are on the right. The contrast at the input gradually changes from positive to negative; the related output abruptly shifts its phase by 180 deg at zero contrast. Before this point the output is linearly related to the input contrast.

constraints. A standard minimization technique applied to the even component shows that the least-squares solution of equation (4) is reached for the following spatial phases of the subunits: $\chi_1 = -2.9$ deg and $\chi_2 = 73.2$ deg, as depicted in Fig. 8(D) by solid circles. The corresponding profiles $Q_1(t)$ and $Q_2(t)$, when com-
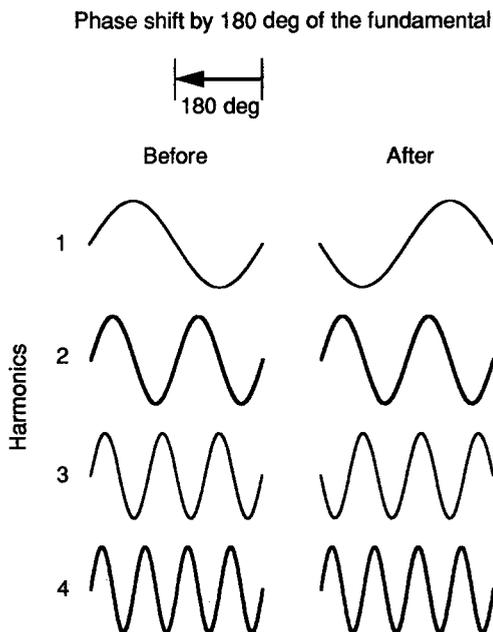
Phase shift by 180 deg of the fundamental

FIGURE 7. Phase shift by 180 deg of the fundamental differently affects odd and even harmonics. Left column: first four harmonics before the phase shift. The amount of shift is shown above by arrow. Right column: the same harmonics after the shift. Notice that the odd (1 and 3) harmonics invert their sign whereas the even (2 and 4) do not change.

bined in accord with equation (4) provide a fit [Fig. 8(D)] that accounts for 90% of the variance of the even component across the range of spatial phases. This is an impressively high percentage because the even component contains a half of the noise in the data, although it accounts for only for 2.9% of the data variance.

With known values for χ_1 and χ_2, equation (3) was solved and the odd components $P_1(t)$ and $P_2(t)$ were also reconstructed. Odd and even components were combined for every spatial phase in accord with equations (3), (4) and (5) to provide the prediction of the quasilinear model shown in Fig. 9. For the full range of spatial phases this prediction reduces the residual variance to 1.3%, 3 times lower than the 3.9% for the linear model. Notice that the quasilinear prediction captures much of the peak feature at spatial phases 135 and 157.5 deg that the other two models failed to predict.

The sums $P_1(t) + Q_1(t)$ and $P_2(t) + Q_2(t)$ represent the exact shapes of the temporal profiles for the subunits; they are shown in Fig. 10(A). These profiles appear to have plausible spatial and temporal relations: (1) the subunits are approximately in spatial quadrature for the spatial frequency optimal for the analyzed cell; (2) the delay between the profiles as estimated for fundamental harmonic is 72 msec which is within the range of the delays between responses of lagged and nonlagged cells in LGN (Saul & Humphrey, 1990). The shape of the profiles is reminiscent of the recordings of spike activity of X-cells, an example of which is presented in Fig. 10(B). Interestingly, the peak-to-trough amplitude of the second subunit is 1.7 times smaller than the amplitude of the first subunit, suggesting unequal gain in the subunits.

DISCUSSION

There are several issues related to the presented analysis that need further discussion.

Precision of the spatial phases of the subunits

The estimates of the subunit spatial phases were obtained by minimization of the residual variance applied to the even component of the signal in equation (4). The residual variance as a function of two spatial phases was a smooth surface with no local minima, and the global minimum was quite narrow at the bottom. A rigorous control of the precision of the phase was done by D. Ferster (personal communication) who applied the described procedure to the recordings from the same cell made for the flicker frequencies 1 and 4 Hz. The spatial phase relations were very close to the estimate given here. The details of this comparison will be described in a forthcoming paper.

Precision of the recordings

The subsequential stages of the analysis presented here impose increasingly tough requirements on the data precision. The linearity of the subunits and the synaptic summation can be proven to a first approximation only for the fundamental, which accounts for the most of the

A
Experimental data

B
Odd harmonics
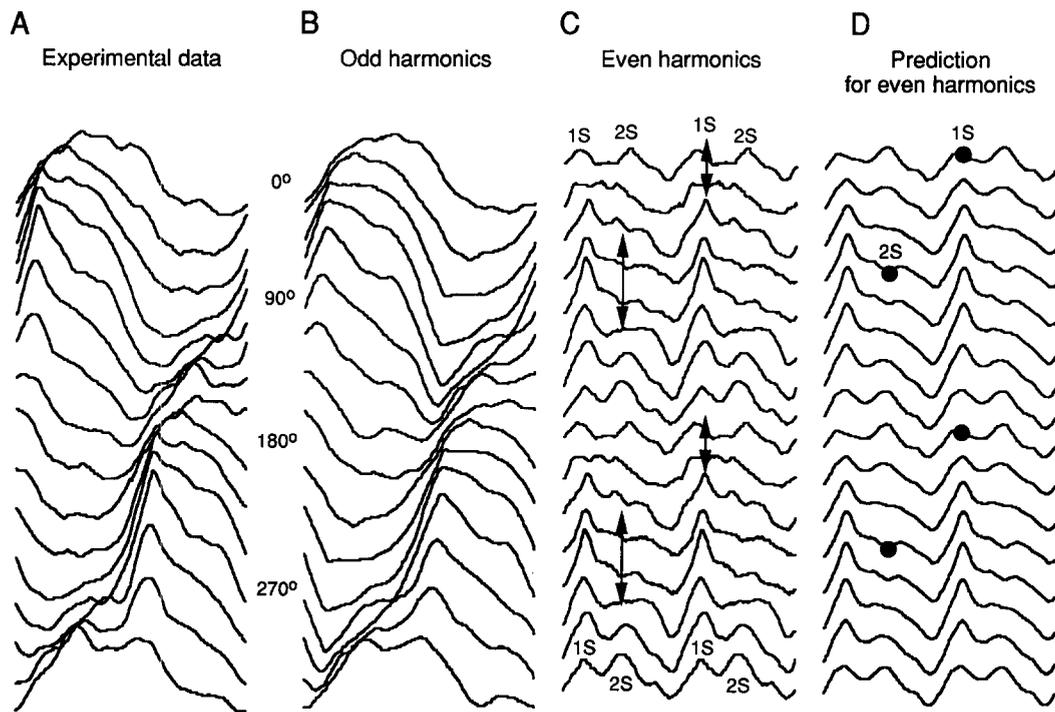
C
Even harmonics

D
Prediction
for even harmonics

FIGURE 8. (A) The extended data for the range of spatial phases from 0 to 360 deg. The responses for the subrange 180–337.5 deg are identical to the responses for the subrange 0–157.5 deg [from Fig. 1(A)] shifted by half-period of the fundamental. (B) The odd components of the data. All features invert sign over the spatial phase range. (C) The even components of the same data magnified vertically by a factor of 2 for illustrative purposes. The peak which is supposedly due to the first subunit is marked 1S. It disappears somewhere between 0 and 22.5 deg. The peak 2S is supposedly linked with the second subunit. It disappears between 45 and 112.5 deg. The estimated ranges for null points are shown by the segments with arrows at the ends. (D) The quasilinear prediction for the even component. Black spots mark the computed null-points for the subunits. The estimates are close to the eyeball estimates from Fig. 7(C).

signal energy. The conclusion that the analyzed cell gets input from two subunits and that the subunits are linear to contrast requires a higher precision, sufficient to analyze the higher harmonics. The most noise-sensitive

part of the analysis is related to the reconstruction of spatial phases of the subunits, which is based on non-linearity of the even harmonics.

The recordings presented in Jagadeesh *et al.* (1993)

A
Experimental data
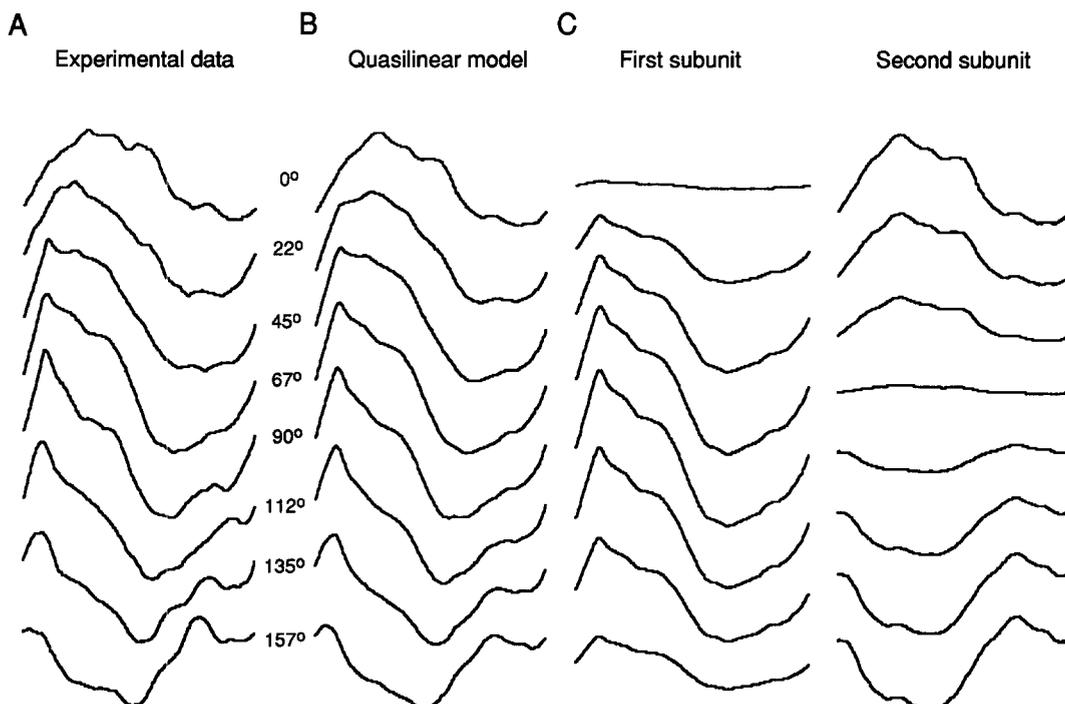
B
Quasilinear model

C
First subunit

Second subunit

FIGURE 9. (A) The data same as in Fig. 1(A). (B) The prediction of the quasilinear model. (C) The signals that come in the simple cell from two subunits. Linear sum of these signals produces the membrane potential recorded in the experiment.

(A)   (B)

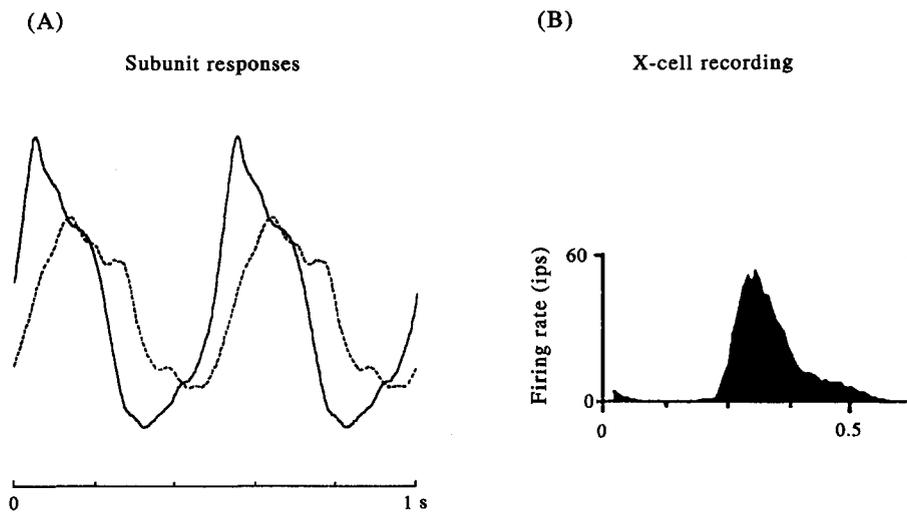Subunit responses   X-cell recording

FIGURE 10. (A) The reconstructed temporal signal profiles of two subunits. The delay between them as measured for fundamental is equal to 72 msec. Their amplitude ratio is 1.7. (B) The recording of action potential from nonlagged X-cell in the lateral geniculate body from Saul and Humphrey (1990, reproduced with permission) resembles the reconstructed profiles.

have a sufficiently low level of noise to allow definitive answers at every stage of the analysis: this was a result of the methodological advantage of the intracellular registration of membrane potentials and the accuracy of the experimenters. The last stage of the analysis also required quite high sampling rate for spatial phases to reconstruct the subunit spatial phases with reasonable precision.

Extracellular recording of action potentials provides an easier access to the activity of neurons. The data obtained with that method, however, contain more noise and include the additional spike-generation nonlinearity at the cell output. It is not clear at this point whether the present analysis would be applicable to action potential data, or, if it is partially applicable, where it fails.

Inputs of the simple cell

One of the main findings in this study is that the response of the analyzed simple cell depends on the signals arriving from two subunits. This conclusion does not imply that the simple cell has no other inputs but that these inputs were not varied in the experiment. For example, the signals of the inputs from the non-stimulated eye (cortical simple cells are mainly binocular) or the lateral inputs necessary for cortical contrast normalization (Heeger, 1992) were constant for all spatial phases.

Contrast linearity of the subunits

The signals that arrive at the cortex from the eye necessarily pass through the LGN. There is good reason, therefore, to expect that distortions of visual information found in the LGN also should be present in the cortex. Measurements of action potentials in LGN cells demonstrate a decelerating nonlinearity in their contrast response: for suprathreshold signals, the number of spikes per second is proportional to the logarithm of contrast (Saul & Humphrey, 1990). How to reconcile this LGN nonlinearity with the contrast linearity of the subunits found in this study? The answer is in the

conditions under which the contrast linearity was evaluated. In the measurements of LGN cell action potentials, the input variable was the contrast of the test grating. Shapley and Victor (1979) established the presence of the nonlinear contrast gain control mechanism in the LGN that sets the gain according to the average contrast over a wide retinal region. Since the contrast of the grating varied, the average contrast also varied and, therefore, the gain control mechanism could nonlinearly distort the response signals. Conversely, the data analyzed in this study were measured for constant contrast of the test grating and, therefore, contrast gain was the same across all the conditions. The stability of the gain is indeed a necessary condition for the linearity of the contrast transduction discovered in this study. It might be interesting to justify this conclusion by direct measurements of contrast transduction in LGN cells while stimulating with a large-field grating of constant contrast and a small test of variable contrast covering the classical receptive field.

Temporal nonlinearity of the subunits

The subunits, according to the presented analysis, are nonlinear in the temporal domain and linear to contrast unless the contrast changes its sign. The simplest nonlinearity of this kind is the absolute value. The half-wave rectifier used in the example in Fig. 5 can be easily expressed via the absolute value as $\text{rect}(s) = (s + \text{abs}(s))/2$.

The ON–OFF dichotomy of LGN cells indicates the involvement of the rectification in the subunit nonlinearity. The bursts of activity of these cells caused by sinusoidal flicker usually have different onset and offset latencies: onset is substantially faster [see Fig. 6 in Saul and Humphrey (1990)]. This is a clear indication that the nonlinearity is more complex than just a simple rectification. The nonlinearity $\text{rect}(\partial\text{rect}(s)/\partial t)$, capturing the latency asymmetry, might be a good candidate to account for the shape of typical signals. This issue, however, is beyond the scope of this study.

CONCLUSION

Intracellular recordings of membrane potentials provide an excellent source of information about the operation of neurons because these recordings are not contaminated by noise or nonlinearities in the spike generation. The set of such intracellular recordings from one directional simple cell from the primary cortex of a cat (the only set currently available from literature) was analyzed. The conclusions of the analysis appeared to be strongly constrained; it is highly unlikely that the derived properties of the cell are a result of a coincidence. The approach proposed in this study can be applied to the analysis of any cells with metric variation of their input stimulus.

REFERENCES

Adelson, E. H. & Bergen, J. R. (1985). Spatiotemporal energy models for the perception of motion. *Journal of the Optical Society of America A, 2,* 284–299.

Albrecht, D. G. & Geisler, W. S. (1991). Motion selectivity and the contrast-response function of simple cells in the visual cortex. *Visual Neuroscience, 7,* 531–546.

Emerson, R. C., Citron, M. C., Vaughn, W. J. & Klein, S. A. (1987). Nonlinear directionally selective subunits in complex cells of cat striate cortex. *Journal of Neurophysiology, 58,* 33–65.

Enroth-Cugell, C. & Robson, J. G. (1966). The contrast sensitivity of retinal ganglion cells of the cat. *Journal of Physiology, London, 187,* 517–552.

Ganz, L. & Felder, R. (1984). Mechanism of directional selectivity in simple neurons of the cat's visual cortex analyzed with stationary flash sequences. *Journal of Neurophysiology, 51,* 294–324.

Heeger, D. J. (1992). Normalization of cell responses in cat striate cortex. *Visual Neuroscience, 9,* 181–197.

Hubel, D. H. & Wiesel, T. N. (1962). Receptive fields, binocular interaction and functional architecture in the cat's visual cortex. *Journal of Physiology, 160,* 106–154.

Jagadeesh, B., Wheat, H. S. & Ferster, D. (1993). Linearity of summation of synaptic potentials underlying direction selectivity in simple cells of the cat visual cortex. *Science, 262,* 1901–1904.

Reichardt, W. (1961). Autocorrelation, a principle for the evaluation of sensory information by the central nervous system. In Rosenblith, W. A. (Eds), *Sensory communication.* New York: Wiley.

Reid, R. C., Soodak, R. E. & Shapley, R. M. (1991). Directional selectivity and spatiotemporal structure of receptive fields of simple cells in cat striate cortex. *Journal of Neurophysiology, 66,* 505–529.

van Santen, J. P. H. & Sperling, G. (1985). Elaborated Reichardt detectors. *Journal of the Optical Society of America A2,* 300–321.

Saul, A. B. & Humphrey, A. L. (1990). Spatial and temporal response properties of lagged and nonlagged cells in cat lateral geniculate nucleus. *Journal of Neurophysiology, 64,* 206–224.

Shapley, R. M. & Victor, J. D. (1979). The contrast gain control of the cat retina. *Vision Research, 19,* 431–434.

Spitzer, H. & Hochstein, S. (1985). A complex-cell receptive-field model. *Journal of Neurophysiology, 53,* 1266–1286.

Tolhurst, D. J. & Dean, A. F. (1991). Evaluation of a linear model of directional selectivity in simple cells of the cat's striate cortex. *Visual Neuroscience, 6,* 421–428.

Watson, A. B. & Ahumada, A. J. Jr (1985). Model of human visual-motion sensing. *Journal of the Optical Society of America A, 2,* 322–342.